



## T-P phase diagram of the Mo–H system revisited



S.N. Abramov<sup>a, b</sup>, V.E. Antonov<sup>a, c, \*</sup>, B.M. Bulychev<sup>b</sup>, V.K. Fedotov<sup>a</sup>, V.I. Kulakov<sup>a</sup>,  
D.V. Matveev<sup>a</sup>, I.A. Sholin<sup>a, b</sup>, M. Tkacz<sup>d</sup>

<sup>a</sup> Institute of Solid State Physics RAS, 142432 Chernogolovka, Russia

<sup>b</sup> Moscow State University, Leninskie Gory, Moscow 119992, Russia

<sup>c</sup> National University of Science and Technology 'MISIS', 119049 Moscow, Leninskii Prosp. 4, Russia

<sup>d</sup> Institute of Physical Chemistry PAS, Kasprzaka 44/52, 01-224 Warsaw, Poland

### ARTICLE INFO

#### Article history:

Received 20 December 2015

Received in revised form

16 February 2016

Accepted 23 February 2016

Available online 4 March 2016

#### Keywords:

Metal hydrides

Phase equilibria

### ABSTRACT

The T-P phase diagram of the Mo–H system studied earlier at hydrogen pressures up to 5.3 GPa and temperatures up to 1200 °C by *in-situ* X-ray diffraction [Y. Fukai et al. Mater. Trans. 44 (2003) 1359] is re-examined at  $P \leq 6$  GPa and  $T \leq 800$  °C using a quenching technique. The formation of the high-temperature *fcc* MoH hydride at  $T > 480$ –570 °C is not confirmed. Instead, the stability region of the low-temperature *hcp* MoH<sub>1.1</sub> hydride is found to grow with pressure. The temperature of its boundary with the region of diluted Mo–H solutions rises with pressure and reaches 800 °C at  $P \approx 5.5$  GPa.

© 2016 Elsevier B.V. All rights reserved.

### 1. Introduction

The greater part of what we know about phase diagrams of the metal–hydrogen systems in the GPa pressure range at temperatures exceeding 400–500 °C has been investigated by the group of Prof. Yuh Fukai using *in situ* synchrotron X-ray diffraction (see Ref. [1] and references therein). The most unusual T-P diagrams were constructed for the Cr–H [2] and Mo–H [3] systems. In these diagrams, the stability region of the high-temperature hydride with a *fcc* ( $\gamma$ ) metal lattice and composition close to CrH or MoH, respectively, lies above the region of diluted solid hydrogen solutions in the *bcc* ( $\alpha$ ) metal. The temperature of the  $\alpha/\gamma$  boundary decreases with decreasing hydrogen pressure, and in order to avoid the crossing of this boundary with the axis  $P = 0$  for the metal without hydrogen, the authors curved it up inside the unexplored interval of low pressures. As a result, a minimum appeared on the boundary curve. In the case of the Cr–H system, a thermodynamical analysis however showed [4] that the  $\alpha/\gamma$  boundary cannot have a minimum.

Consequently, the position of the  $\alpha/\gamma$  boundary in the Cr–H system proposed in [2] cannot be correct. A similar analysis of phase relations in the Mo–H system shows that the  $\alpha/\gamma$  boundary in its T-P diagram cannot have a minimum either and therefore this

boundary was not correctly constructed in [3].

The present paper was initially aimed at establishing the correct position of the  $\alpha/\gamma$  boundary in the Mo–H system by using a quenching technique. The Mo–H system was better suited for such an investigation than the Cr–H system because of the much lower temperatures of 480–570 °C of the  $\alpha/\gamma$  boundary [3]. Besides, the  $\gamma$ -CrH hydride has long been known and rather thoroughly studied (see [5] and references therein), whereas the  $\gamma$ -MoH hydride was only observed by X-ray diffraction in Ref. [3] therefore its synthesis and a more detailed examination looked an attractive task.

Surprisingly, our experiments demonstrated that  $\gamma$ -MoH is not formed at temperatures up to 800 °C and hydrogen pressures up to 6 GPa. Instead, the stability region of the high-pressure low-temperature *hcp* ( $\epsilon$ ) molybdenum hydride [6] with an H/Mo atomic ratio of  $x \approx 1.1$  was found to grow with increasing pressure, and we constructed the  $\epsilon/\alpha$  boundary ascending approximately linearly from 400 °C at 3 GPa to 800 °C at 5.5 GPa.

### 2. Samples preparation and experimental details

The starting material was a 0.25 mm polycrystalline foil of 99.98% Mo metal. Platelets of about 5 mm in diameter cut out of this foil were exposed to gaseous hydrogen at a pre-selected temperature and pressure and then rapidly cooled (quenched) to the liquid N<sub>2</sub> temperature to prevent further changes in the hydrogen content of the Mo–H samples thus synthesized. The crystal

\* Corresponding author.

E-mail address: [antonov@issp.ac.ru](mailto:antonov@issp.ac.ru) (V.E. Antonov).

structure of these Mo–H samples was examined by X-ray diffraction at ambient pressure and  $T = 85$  K. The hydrogen content of the samples was determined by hot extraction.

The hydrogenation of molybdenum was carried out in copper cells similar to those proposed in Ref. [7]. The design of our cells is schematically shown in Fig. 1. Using a quasihydrostatic Toroid-type high-pressure chamber [8], the cell was first compressed to 0.6–1.5 GPa and heated to 250–400 °C to decompose the compound served as internal source of hydrogen. In the experiments at temperatures up to 450 °C, this compound was  $\text{AlH}_3$ ; at higher temperatures,  $\text{NH}_3\text{BH}_3$  was used (in heating above 200 °C,  $\text{AlH}_3$  decomposes to Al metal and  $\text{H}_2$  gas [7]; the only products of decomposition of  $\text{NH}_3\text{BH}_3$  are solid BN and  $\text{H}_2$  gas [9]). The cell always had the external diameter 8.5 mm and the height 6 mm, while the thickness of its walls varied from 0.7 mm in the experiments at 400 °C to 1.5 mm at 800 °C. The increase in the wall thickness reduced the hydrogen losses and warranted the presence of gaseous hydrogen in the cell for 2 days at 400 °C and for 30 min at 800 °C. The pressure in the cell was determined with an accuracy of  $\pm 0.3$  GPa; the accuracy of determining the temperature varied from  $\pm 15$  °C at 400 °C to  $\pm 20$  °C at 800 °C (see Ref. [10] for details).

Our cells also have much in common with those elaborated by the group of Prof. Fukai [11]. The most significant differences are that the Japanese researchers use thermal decomposition of  $\text{LiAlH}_4$  [11] or the reaction between  $\text{NaBH}_4$  and  $\text{Ca}(\text{OH})_2$  [2,3] to produce hydrogen inside the cell, and the walls of the cell are made of NaCl. We prefer copper to rock salt because our experiments showed that copper is much less permeable to hydrogen at pressures above 3–5 GPa and temperatures above 500 °C.

In our experiments, the sample hydrogenated in an  $\text{H}_2$  atmosphere at given temperature and pressure was then cooled (quenched) together with the high-pressure chamber to room temperature in 15–20 s and further to  $\sim 80$  K in 20–30 min. The pressure was then released; the chamber was disassembled under liquid nitrogen; the sample was retrieved from the cell and stored in liquid  $\text{N}_2$  until the measurements.

Each hydrogenated sample was examined by X-ray diffraction at 85 K with a Siemens D500 diffractometer using  $\text{Cu K}\alpha$  radiation selected by a diffracted beam monochromator. The diffractometer was equipped with a home-designed nitrogen cryostat that permitted the samples to be loaded without any intermediate warming. The obtained diffraction patterns were analyzed using POWDERCELL2.4 software.

The thermal stability and the total hydrogen content of the samples were determined by thermodesorption of hydrogen into a

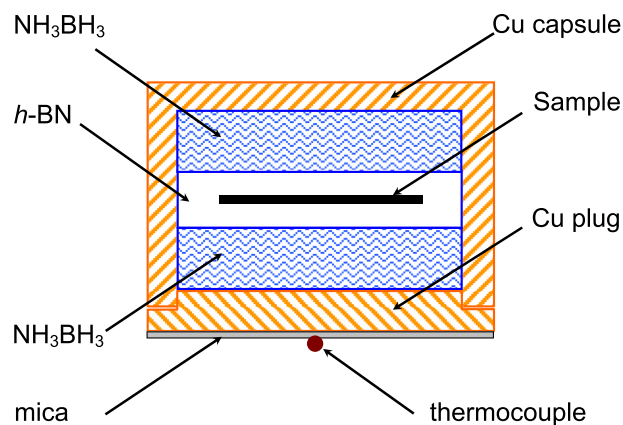


Fig. 1. Schematic diagram of the high-pressure cell using aminoborane  $\text{NH}_3\text{BH}_3$  as a solid hydrogen source.

pre-evacuated measuring system in the regime of heating from 85 K to 660 °C at a rate of 10 °C/min. The mass of the analyzed probe was a few milligrams; the accuracy in determining the atomic ratio  $x = \text{H}/\text{Mo}$  varied from  $\pm 0.003$  at  $x \approx 0.02$  to  $\pm 0.03$  at  $x > 0.5$ . The method is described in more detail in Ref. [12].

### 3. Results and discussion

The  $T$ - $P$  phase diagram of the Mo–H system constructed in Ref. [3] is depicted in Fig. 2 by the thick lines. At the bottom of this figure, the dash-dotted lines show the curves of formation and decomposition of  $\epsilon$  molybdenum hydride determined in our earlier work [13] from the midpoints of the steps in the isotherms and isobars of electrical resistance. In view of the large hysteresis of the  $\alpha \leftrightarrow \epsilon$  transformation, it should be mentioned here that the pressure of equilibrium between a dilute hydrogen solution and a hydride is always closer to the decomposition pressure of the hydride than to the pressure of its formation (see [14] for discussion and explanation). As one can see, the  $\epsilon \rightarrow \alpha$  curve from [13] is in fair agreement with the  $\alpha/\epsilon$  boundary from [3].

#### 3.1. Minimum on the $\alpha/\gamma$ boundary constructed in [3].

As seen from Fig. 2, the  $\alpha/\gamma$  boundary constructed in [3] has a minimum at  $P \approx 2.3$  GPa and  $T \approx 480$  °C. An analysis of volume effects accompanying the  $\alpha \rightarrow \gamma$  transition however shows that the boundary cannot have a minimum if it represents equilibrium between the dilute Mo–H solution and the stoichiometric  $\gamma$ -MoH hydride.

In fact, as can easily be demonstrated [4], every line

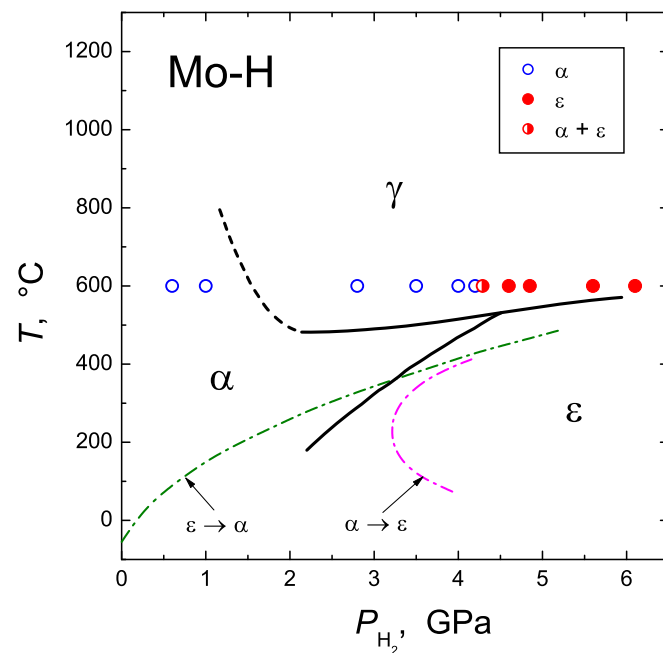


Fig. 2. Experimental  $T$ - $P$  phase diagram of the Mo–H system. The thick lines are constructed in Ref. [3] using in situ X-ray diffraction. These lines divide the diagram into stability regions of the  $\alpha$  phase (dilute solid hydrogen solutions in  $bcc$  Mo), the  $\epsilon$  phase (molybdenum hydride with a  $hcp$  metal lattice and composition close to MoH) and the  $\gamma$  phase, which has a  $fcc$  metal lattice and is supposed to be [3] a nearly stoichiometric hydride MoH. The dash-dotted lines show the conditions of formation ( $\alpha \rightarrow \epsilon$  transition) and decomposition ( $\epsilon \rightarrow \alpha$  transition) of the  $\epsilon$  molybdenum hydride according to the measurements of electrical resistance [13]. The circles indicate the synthesis pressures and phase compositions of the Mo–H samples loaded with hydrogen at 600 °C in the present paper.

representing a transition between two different Me–H phases in the  $T$ - $P$  diagram of a binary Me–H system should obey the analog of Clapeyron's equation:

$$dT/dP = \Delta V/\Delta S,$$

where  $\Delta V$  and  $\Delta S$  are the total volume and entropy change of the system undergoing the transition at given  $T$  and  $P$ . At the point of minimum,  $dT/dP = 0$  and this requires  $\Delta V = 0$ .

In the case of the Mo–H system,  $\Delta V = V_\gamma - V_\alpha - V_{\text{gas}} = \Delta V_{\alpha \rightarrow \gamma} - V_{\text{gas}} = 0$ , where  $V_\gamma$  and  $V_\alpha$  are the molar volumes of the  $\alpha$  and  $\gamma$  phases and  $V_{\text{gas}}$  is the volume of molecular hydrogen absorbed by 1 mol of molybdenum in the course of the  $\alpha \rightarrow \gamma$  transition. The absorbed hydrogen increases the H/Mo ratio of the sample by:

$$\Delta x_{\alpha \rightarrow \gamma} = 2V_{\text{gas}}/V_{\text{H}_2} = 2\Delta V_{\alpha \rightarrow \gamma}/V_{\text{H}_2}, \quad (1)$$

where  $V_{\text{H}_2}$  is the molar volume of gaseous  $\text{H}_2$ . According to the X-ray results of Ref. [3],  $\Delta V_{\alpha \rightarrow \gamma} \approx 2.7 \text{ \AA}^3/\text{atom Mo} \approx 1.6 \text{ cm}^3/\text{mol Mo}$  and does not change along the  $\alpha/\gamma$  boundary. At the point of minimum on this boundary (2.3 GPa, 480 °C), the  $\text{H}_2$  gas has  $V_{\text{H}_2} = 12.84 \text{ cm}^3/\text{mol H}_2$  [15]. Substituting these values of  $\Delta V_{\alpha \rightarrow \gamma}$  and  $V_{\text{H}_2}$  in Eq. (1) gives  $\Delta x_{\alpha \rightarrow \gamma} \approx 2 \cdot 1.6/12.84 = 0.25$ . Since the hydrogen solubility in the  $\alpha$  phase is limited to a few atomic per cent [3,13], the hydrogen content of the  $\gamma$  phase cannot therefore exceed  $x_\gamma = x_\alpha + \Delta x_{\alpha \rightarrow \gamma} \approx 0.3$ . This is three times less than  $x_\gamma \approx 1$  proposed in [3].

The formation of  $\gamma$ - $\text{MoH}_{0.3}$  from the diluted  $\alpha$  solution is however very unlikely because this would lead to the volume expansion  $\Delta V_{\alpha \rightarrow \gamma}/\Delta x_{\alpha \rightarrow \gamma} \approx 2.7/0.3 = 9 \text{ \AA}^3/\text{atom H}$  whereas the volume effect of hydrogen absorption by transition metals is of the order of 2–3  $\text{\AA}^3/\text{atom H}$  in all studied cases [1].

Consequently, we face the alternative: either the correct  $\alpha/\gamma$  boundary has no minimum, or the  $\gamma$  phase is not a binary Mo–H hydride. The latter could not be excluded because the MoH composition for the  $\gamma$  phase was deduced in [3] from  $\Delta V_{\alpha \rightarrow \gamma} \approx 2.7 \text{ \AA}^3/\text{atom Mo}$  and never examined experimentally. First of all, we attempted to locate the  $\alpha/\gamma$  boundary.

### 3.2. Isotherm of the hydrogen solubility in molybdenum at 600 °C

To begin with, we constructed an isotherm of hydrogen solubility in molybdenum at a temperature of 600 °C. As seen from Fig. 2, this isotherm lies in the stability range of  $\gamma$ -MoH determined in [3]. The samples were exposed to an  $\text{H}_2$  atmosphere for 30 min at the conditions indicated by the circles in this figure and quenched to 80 K. An X-ray diffraction study showed that none of the quenched samples contained  $\gamma$ -MoH at ambient pressure and 85 K. The filled circles stand for the samples that were single-phase  $\epsilon$  hydride according to the X-ray analysis and had H/Mo  $\approx 1.1$  according to the thermodesorption measurements. The open circles are for the single-phase samples of dilute solid hydrogen solutions in bcc Mo (the  $\alpha$  phase) with the hydrogen content reaching H/Mo  $\sim 0.01$  at 4.2 GPa. The sample indicated by the half-filled circle consisted of a mixture of bcc Mo and  $\epsilon$ - $\text{MoH}_{1.1}$ .

The resulting isotherm of hydrogen solubility in molybdenum at 600 °C is presented in Fig. 3. Typical curves of hydrogen desorption from different Mo–H samples are shown in Fig. 4.

Because of the hysteresis effects accompanying phase transformations in the Mo–H system, the interpretation of the phase composition of the samples depends on the path of their synthesis. Particularly, the three Mo–H samples synthesized at 600 °C and hydrogen pressures up to 2.8 GPa (see Fig. 2) were first compressed to the chosen pressure at room temperature and further heated to

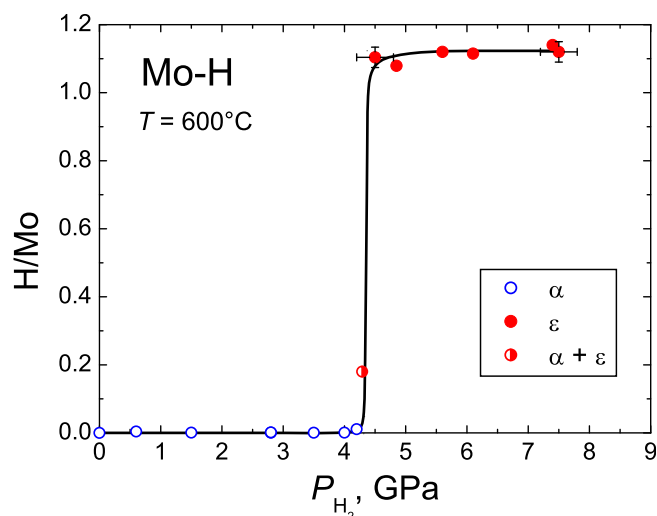


Fig. 3. Isotherm of the hydrogen solubility in molybdenum at 600 °C.

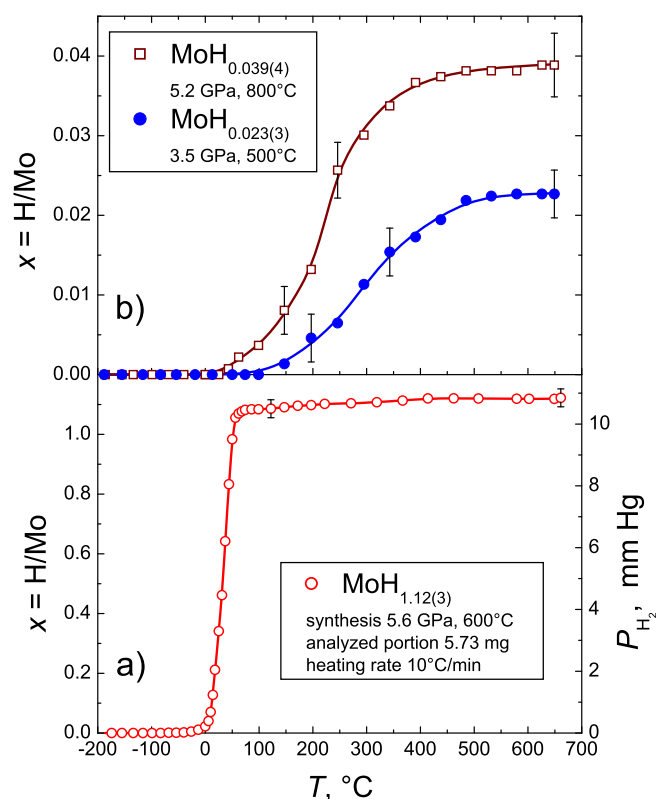


Fig. 4. Temperature dependences of the amount of hydrogen released from Mo–H samples heated at 10 °C/min in a closed-volume, pre-evacuated measuring system. (a) Single-phase sample of hcp ( $\epsilon$ ) molybdenum hydride; the right scale shows the gas pressure in the measuring system. (b) Two samples synthesized in the  $T$ - $P$  range of stability of dilute hydrogen solutions in bcc ( $\alpha$ ) molybdenum.

600 °C in approximately 1 h. The samples synthesized at  $P \geq 3.5$  GPa were primary transformed to the single-phase state of  $\epsilon$ - $\text{MoH}_{1.1}$  hydride by a 1 day exposure to the chosen  $\text{H}_2$  pressure and a lower temperature of 300–350 °C (the synthesis of  $\epsilon$ - $\text{MoH}_{1.1}$  was carried out in the  $T$ - $P$  region on the right of the dash-dotted curve of the  $\alpha \rightarrow \epsilon$  transition determined in [13]; the formation of the  $\epsilon$  hydride under these conditions was proved in separate experiments). The samples of  $\epsilon$ - $\text{MoH}_{1.1}$  thus obtained were then heated to 600 °C

without changing the pressure; the heating took about half an hour.

The presence of  $\epsilon$ -MoH<sub>1.1</sub> in the samples quenched from 600 °C and  $P \geq 4.3$  GPa contradicts results of Ref. [13] predicting that this hydride should decompose on heating the samples above the line of the  $\epsilon \rightarrow \alpha$  transition (dash-dotted curve in Fig. 2) at much lower temperatures.

The absence of  $\gamma$ -MoH in our quenched samples was not necessarily at variance with the  $T$ - $P$  diagram of the Mo–H system constructed in Ref. [3] and shown in Fig. 2, because one could not exclude that:

- The samples quenched from the pressures up to 4.2 GPa lost nearly all hydrogen while crossing the  $\alpha$  region.
- At  $T = 600$  °C and  $P \geq 4.3$  GPa, our samples were single-phase  $\gamma$  hydride with  $H/Me \approx 1.1$ . In the course of quenching, this hydride however transformed to the  $\epsilon$ -MoH<sub>1.1</sub> phase, which was more thermodynamically stable at lower temperatures.

### 3.3. Revised $T$ - $P$ diagram of the Mo–H system

To learn more about phase transformations in the Mo–H system, we synthesized additional samples at hydrogen pressures from 3.3 to 5.7 GPa and temperatures from 400 to 800 °C. The duration of the synthesis varied from 4 h at 400 °C to 20 min at 800 °C. Prior to this treatment, each sample had been transformed to the single-phase state of  $\epsilon$ -MoH<sub>1.1</sub> hydride by a 1 day exposure to the chosen H<sub>2</sub> pressure and a temperature of 250–350 °C and then heated to the desired temperature in 20–40 min.

Phase compositions of the synthesized samples determined by X-ray diffraction are shown in Fig. 5. As one can see,  $\gamma$ -MoH is not detected in any of the samples. The points of decomposed  $\epsilon$ -MoH<sub>1.1</sub> (open circles) lie straight above the points of single-phase samples of  $\epsilon$ -MoH<sub>1.1</sub> (filled circles). This suggests that  $\gamma$ -MoH or any other hydride, if it were formed under the conditions indicated by the open circles, would immediately fall into the stability region of the  $\epsilon$ -hydride in the course of quenching and would not cross a wide

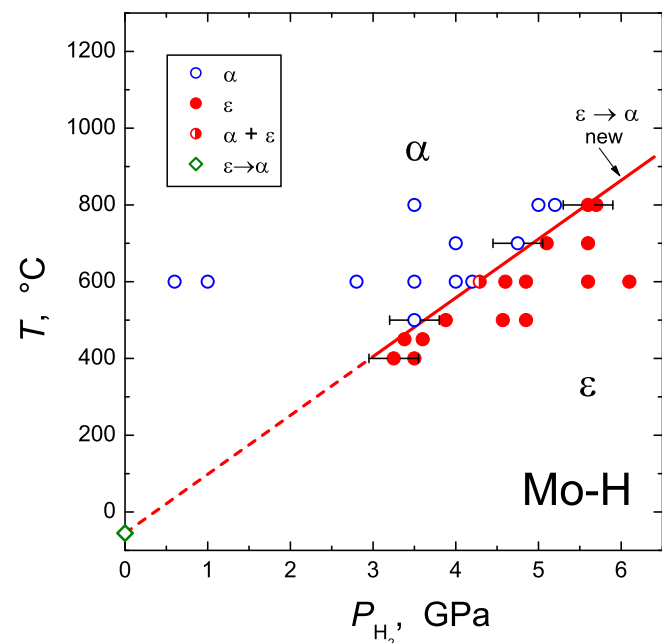


Fig. 5.  $T$ - $P$  phase diagram of the Mo–H system according to results of the present paper.

temperature interval of the  $\alpha$  phase with a low hydrogen concentration. Quenching the hypothetical high-pressure hydride might transform it to  $\epsilon$ -MoH<sub>1.1</sub> with similar hydrogen content, but there were no thermodynamical reasons for the sample to lose hydrogen. We could thus conclude that the samples of  $\epsilon$ -MoH<sub>1.1</sub> heated and exposed to the temperature and pressure of the open circles should have lost most hydrogen and transformed to the  $\alpha$  phase.

In the  $T$ - $P$  diagram of the Mo–H system, the line of the  $\epsilon \rightarrow \alpha$  transition should lie above the experimental points for the  $\epsilon$  hydride (filled circles in Fig. 5) and below the points for the  $\alpha$  solutions (open circles). Within our accuracy of determining the hydrogen pressure  $\pm 0.3$  GPa and temperature  $\pm 20$  °C, this boundary can be represented by a straight line passing through the point of decomposition of  $\epsilon$ -MoH<sub>1.1</sub> at ambient pressure (the open diamond at  $T = -55$  °C; data of [6]). The slope of the line is  $dT/dP = 155$  (5) °C/GPa.

The absence of formation of the  $\gamma$  phase in the  $T$ - $P$  region above the  $\epsilon/\gamma$  boundary constructed in Ref. [3] suggests that this phase does not form at any conditions, including the region above the  $\alpha/\gamma$  boundary at lower hydrogen pressures. The  $\epsilon$  phase is therefore the only hydride that undoubtedly exists in the Mo–H system at pressures up to 6 GPa.

### 3.4. Composition and lattice parameters of the $\epsilon$ and $\alpha$ phases in the Mo–H system

Results of our studies of the hydrogen content and crystal structure of quenched single-phase samples of the  $\epsilon$  molybdenum hydride are presented in Figs. 6 and 7.

As seen from the bottom panel of Fig. 6, the hydrogen content of the  $\epsilon$  hydride does not depend on the synthesis temperature and pressure within the experimental error and its mean value equals to  $x = 1.10$  (3). Interestingly, the origin of the “overstoichiometric” composition  $x > 1$  of the  $\epsilon$  molybdenum hydride has not been understood yet. Particularly, a quenched sample of this hydride having  $x = 1.19$  (5) according to the volumetric analysis was earlier studied by powder neutron diffraction and shown to contain only  $x = 0.95$  (5) of hydrogen, which occupied octahedral interstices in the  $hcp$  molybdenum lattice [16]. In order to determine the location of the missing  $\delta x \approx 0.2$  of hydrogen, model structures of the hydride with vacancies in the  $hcp$  molybdenum lattice and with hydrogen atoms partly occupying tetrahedral interstitial sites were also analyzed. However, fitting the experimental diffraction pattern

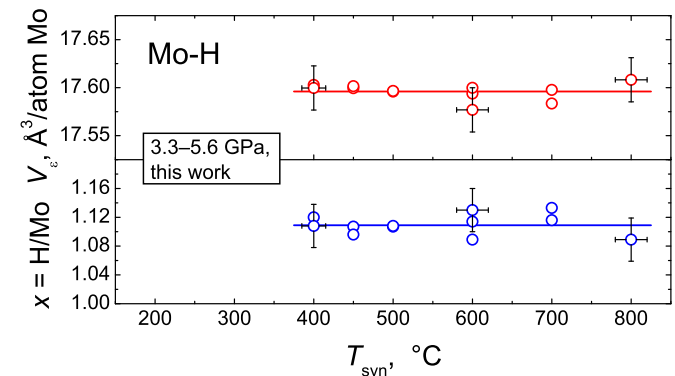
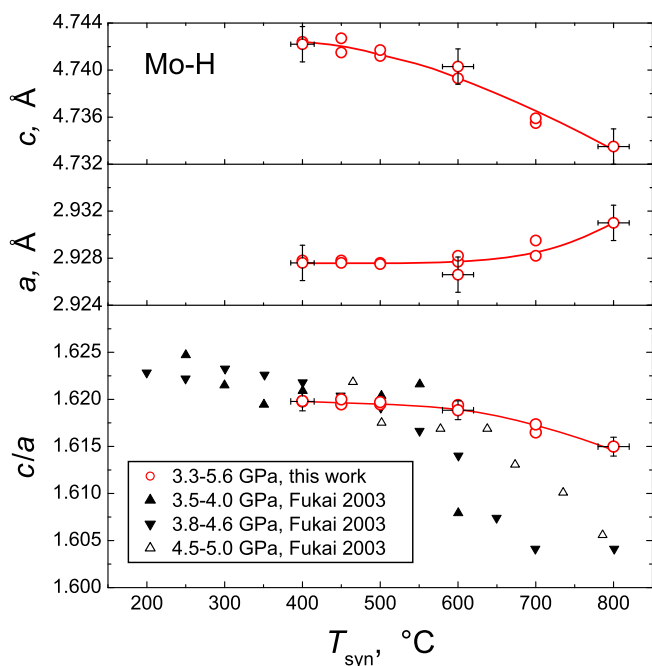


Fig. 6. The hydrogen content  $x = H/Mo$  and atomic volume  $V_\epsilon = \sqrt{3}/4 a^2 c$  of the  $hcp$   $\epsilon$  hydride of molybdenum as a function of the synthesis temperature. The samples were loaded with hydrogen at pressures from 3.3 to 5.6 GPa and quenched to the liquid N<sub>2</sub> temperature. The hydrogen content of the quenched samples was determined by thermal desorption in vacuum. The crystal structure was examined by X-ray diffraction at ambient pressure and  $T = 85$  K.



**Fig. 7.** The lattice parameters  $a$  and  $c$  and the  $c/a$  ratio of the  $\epsilon$  hydride of molybdenum as a function of the synthesis temperature. The triangles show results of in situ measurements of Ref. [3]. The circles show results for the quenched Mo–H samples studied at ambient pressure and  $T = 85$  K in the present paper.

converged to the zero concentrations of both the vacancies and tetrahedrally coordinated H atoms.

Along with the hydrogen content, the atomic volume  $V_\epsilon = \frac{\sqrt{3}}{4}a^2c$  of quenched samples of the  $\epsilon$  molybdenum hydride also shows no dependence on the synthesis temperature and pressure. As one can see from the upper panel of Fig. 6, the mean value of this volume is  $V_\epsilon = 17.60(2) \text{ \AA}^3/\text{atom Mo}$ . It is greater than the atomic volume  $V_0 = a_0^3/2 = 15.52(1) \text{ \AA}^3/\text{atom Mo}$  of bcc molybdenum by  $\Delta V_{\alpha \rightarrow \epsilon} = 2.08(2) \text{ \AA}^3/\text{atom Mo}$ , which agrees with the value of  $\Delta V_{\alpha \rightarrow \epsilon} = 2.1 \text{ \AA}^3/\text{atom Mo}$  determined at temperatures 200–600 °C and pressures 2.5–4.5 GPa in the in situ measurements of Ref. [3].

The  $a$  and  $c$  parameters of the  $hcp$  metal lattice of quenched  $\epsilon\text{-MoH}_{1.1}$  samples do not depend on the synthesis pressure either, but they noticeably vary with the synthesis temperature. As seen from Fig. 7, the  $c$  parameter decreases and the  $a$  parameter increases with increasing  $T_{\text{syn}}$  that leads to the gradual decrease in the  $c/a$  ratio from 1.620(1) at  $T_{\text{syn}} = 400$  °C to 1.615(1) at  $T_{\text{syn}} = 800$  °C. The  $c/a$  ratios measured under equilibrium conditions at high hydrogen pressures [3] also gradually decrease with increasing temperature, only the dependence is steeper (triangles in Fig. 7). The  $c/a$  versus  $T_{\text{syn}}$  dependence for our quenched samples therefore partly inherits the behavior of this equilibrium dependence.

The hydrogen concentration in the dilute  $\alpha$  solutions is maximal near the  $\epsilon \rightarrow \alpha$  boundary (solid line in Fig. 5) and monotonically increases along this boundary from  $x \sim 0.01\text{--}0.02$  at 500 °C to  $x \sim 0.04$  at 800 °C. According to the X-ray diffraction data, the quenched samples indicated by open circles in Fig. 5 were single-phase  $\alpha$  solutions at  $T = 85$  K and ambient pressure. The lattice parameter of their bcc molybdenum sublattice increased with the hydrogen concentration and reached  $a = 3.148(2) \text{ \AA}$  at  $x = 0.039(3)$ . Compared to  $a_0 = 3.143(1) \text{ \AA}$  of molybdenum at  $T = 85$  K, this corresponds to the hydrogen-induced increase in the Mo volume at a rate of the order of  $[a^3/2 - a_0^3/2]/x \sim 2 \text{ \AA}^3/\text{atom H}$ , which is typical of hydrogen solutions in d-metals [1].

Most of the  $\alpha$  samples examined by X-ray diffraction were first

transformed to  $\epsilon\text{-MoH}_{1.1}$  and further brought to the state of the  $\alpha$  solution by the reverse  $\epsilon \rightarrow \alpha$  transformation. The single-phase composition of the  $\alpha$  samples therefore evidences that this reverse transformation was fully completed. The completeness of the  $\epsilon \rightarrow \alpha$  transformation also follows from the thermal desorption experiments. As seen from Fig. 4, the curves of hydrogen desorption from the  $\alpha$  and  $\epsilon$  samples are considerably different and the step at 0–60 °C characteristic of decomposition of the  $\epsilon$  hydride (Fig. 4a) is absent in the curves for the  $\alpha$  samples (Fig. 4b).

### 3.5. Disagreement between results of the present paper and Ref. [13]

As the line of hydride decomposition is likely to be close to the equilibrium line [14], one could expect that the curves of the  $\epsilon \rightarrow \alpha$  transition in the Mo–H system constructed by different methods would well agree with each other. As seen from Fig. 8, at temperatures up to 325 °C, the experimental points of this transition determined from measurements of the electrical resistance [13] do agree with the line “ $\epsilon \rightarrow \alpha$  new” produced in the present work using the quenching technique. At higher temperatures, however, the points of Ref. [13] more and more deviate from the new  $\epsilon \rightarrow \alpha$  line toward higher pressures and the difference reaches about 1.7 GPa at 500 °C.

A possible explanation of this discrepancy is as follows. In contrast to the present work, the hydrogen compressed in [13] was always in contact with silicon oil used as a “hydraulic gate” preventing hydrogen losses from the high-pressure cell made of Teflon. Our earlier experiments have shown [17] that the partial pressure of the silicon oil vapor in molecular hydrogen is below the experimental error of 0.3 GPa at temperatures up to 300 °C and the total gas pressures up to 6 GPa. One can, however, speculate that the partial pressure of silicon oil rapidly grows at temperatures above 300 °C. If it reaches 1.7 GPa at 500 °C and the total gas

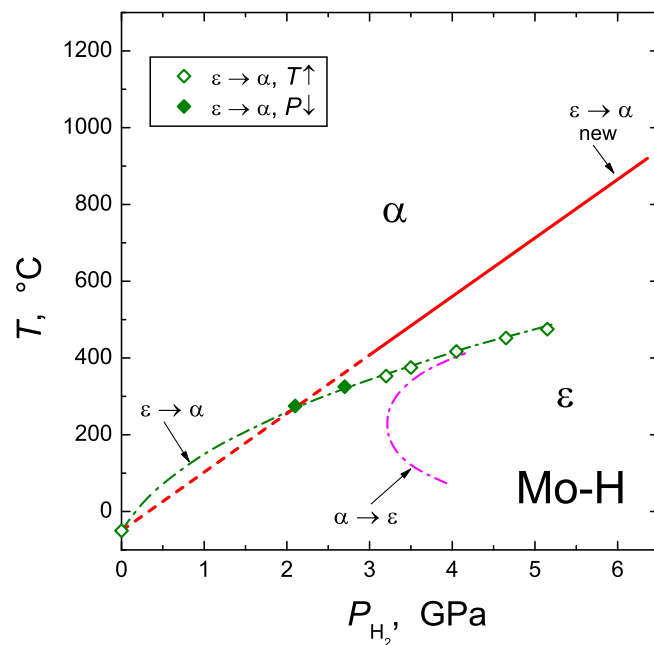


**Fig. 8.** The line of the  $\epsilon \rightarrow \alpha$  transition in the Mo–H system constructed in the present paper (straight line labeled “ $\epsilon \rightarrow \alpha$  new”) in comparison with the lines of the  $\epsilon \rightarrow \alpha$  and  $\alpha \rightarrow \epsilon$  transitions [13] shown by the dash-dotted curves. The points of the  $\epsilon \rightarrow \alpha$  transition determined in Ref. [13] are indicated by the filled and open diamonds, correspondingly, for the experiments with decreasing pressure at constant temperature and increasing temperature at constant pressure.

pressure 5 GPa, this will explain the difference in the pressures of the  $\epsilon \rightarrow \alpha$  transition in the Mo–H system determined in the present work and Ref. [13].

### 3.6. Disagreement between results of the present paper and Ref. [3]

An analysis of experimental data of Ref. [3] led us to the conclusion that the high-temperature  $\gamma$  phase discovered in that work could not be a binary Mo–H compound. Instead, it was a product of a chemical reaction of molybdenum with the debris of the high-pressure cell in the presence of molecular hydrogen. To substantiate this conclusion, we have to consider the results of Ref. [3] in more detail.

Fig. 9 shows the experimental points used in Ref. [3] to construct the phase boundaries labeled  $\alpha/\gamma$ ,  $\alpha/\epsilon$  and  $\epsilon/\gamma$ . A few series of these points were obtained in the course of a step-wise heating of the sample in an atmosphere of molecular hydrogen at a constant ram load. At each temperature, the sample was equilibrated for 10–30 min and examined by X-ray diffraction using synchrotron radiation.

The transition of the  $\alpha$  phase (open squares) to the  $\gamma$  phase (filled squares) was rather fast and its temperature interval did not exceed 50–100 °C. The  $\alpha/\gamma$  boundary showed nearly no baric dependence in the experimental pressure range above 2 GPa, but the authors of Ref. [3] arbitrarily curved it upward at lower pressures in order to avoid the crossing of this boundary with the axis  $P = 0$  for the metal without hydrogen. As shown in Section 3.1, the resulting minimum on the  $\alpha/\gamma$  boundary is at variance with thermodynamics, if the  $\gamma$  phase is a binary Mo–H hydride. If the  $\gamma$  phase is supposed to be a product of a chemical reaction of molybdenum with some other substance present in the high-pressure cell, this

removes the limitations on the behavior of the  $\alpha/\gamma$  boundary at pressures below 2 GPa.

The  $\epsilon$  hydride (filled triangles in Fig. 9) was produced in Ref. [3] in the three runs, each starting from the  $T$ - $P$  region on the right of the dash-dot curve of the  $\alpha \rightarrow \epsilon$  transition constructed earlier [13]. The merged  $\alpha/\gamma$  and  $\epsilon/\gamma$  boundary at about 520–530 °C shows the onset of the  $\epsilon \rightarrow \gamma$  transition in the course of heating [3]. The transition was rather sluggish, and the filled squares in Fig. 9 only indicate the presence of the  $\gamma$  phase in the corresponding samples without saying if the  $\epsilon \rightarrow \gamma$  transition is complete or not. Nevertheless, the limiting temperatures of persistence of the  $\epsilon$  hydride can roughly be estimated from the temperature dependences of the  $c/a$  ratios of its  $hcp$  lattice, which were measured in Ref. [3] for the samples heated to about 600 °C at 4.0 GPa and to about 800 °C at 4.6 and 5.0 GPa (triangles in the bottom panel of Fig. 7). These three upper points are connected with the hatched line in Fig. 9.

According to [3], the  $\epsilon$  hydride thus did not disappear in heating the samples across the merged  $\alpha/\gamma$  and  $\epsilon/\gamma$  boundary at about 520–530 °C. Instead, it persisted up to the considerably higher temperatures indicated by the hatched line. The two-phase interval of the  $\epsilon \rightarrow \gamma$  transition (the distance between the  $\alpha/\gamma$ – $\epsilon/\gamma$  boundary and the hatched line) steeply increased from less than 100 °C at 4.0 GPa to more than 250 °C at 4.6–5.0 GPa. This can be explained under the assumption that the kinetics of the  $\alpha \rightarrow \gamma$  transition was much faster than that of the  $\epsilon \rightarrow \gamma$  transition, so the samples completely transformed to the  $\gamma$  phase soon after heating above the “ $\epsilon \rightarrow \alpha$  new” transition line constructed in the present work.

The  $T$ - $P$  region of formation of the dilute  $\alpha$  solutions (open squares in Fig. 9) agrees with the dash-dot curve of the  $\alpha \rightarrow \epsilon$  transition determined earlier [13]. The  $\alpha/\epsilon$  boundary drawn in Ref. [3] between these points and the points of formation of the  $\epsilon$  phase (filled triangles) therefore represents the line of the  $\alpha \rightarrow \epsilon$  transition. In view of the large baric hysteresis of the  $\alpha \leftrightarrow \epsilon$  transformation, the shift of this  $\alpha/\epsilon$  boundary to higher pressures relative to the “ $\epsilon \rightarrow \alpha$  new” transition line is quite reasonable.

There seems to be only one experimental result of Ref. [3] that disagrees with the “ $\epsilon \rightarrow \alpha$  new” line and cannot be explained under the assumption that the  $\gamma$  phase is not a binary Mo–H hydride. This is the appearance of the  $\alpha$  phase in the  $\epsilon$  samples heated to 500 °C at 3.9 and 4.1 GPa (half-filled triangles in Fig. 9). This result was not however reproduced in our experiments. As one can see from Fig. 10, the sample prepared at 500 °C and 3.9 GPa was composed of the  $\epsilon$ -MoH<sub>1.11(3)</sub> hydride and contained no traces of the  $\alpha$  and  $\gamma$  phases.

## 4. Conclusions

Results of the present paper show that in the range of hydrogen pressures up to 6 GPa and temperatures up to 800 °C, molybdenum and hydrogen only form two phases, dilute  $\alpha$  solutions of hydrogen in  $bcc$  Mo and  $\epsilon$  hydride with the  $hcp$  metal lattice. The temperature of the  $\epsilon \rightarrow \alpha$  transition increases with pressure from 400 °C at 3 GPa to 800 °C at 5.5 GPa. The hydrogen concentration in the solid  $\alpha$  solutions is maximal near the  $\epsilon \rightarrow \alpha$  boundary and increases along this boundary from the atomic ratio H/Mo of  $x \sim 0.01$ – $0.02$  at 500 °C to  $x \sim 0.04$  at 800 °C. The composition of the  $\epsilon$  hydride is close to MoH<sub>1.10</sub> and does not depend on the synthesis temperature and pressure within the experimental error of  $\delta x = \pm 0.03$ . Quenched samples of the  $\epsilon$  hydride examined by X-ray diffraction at ambient pressure and  $T = 85$  K had the axial ratios of the  $hcp$  metal lattice varying from  $c/a = 1.620$  (1) to 1.615 (1) with the increase in the synthesis temperature from 400 to 800 °C. The atomic volume  $V_\epsilon = \sqrt{3}a^2c = 17.60$  (2) Å<sup>3</sup>/atom Mo showed no dependence on the synthesis conditions.

Compared to earlier studies of the Mo–H system, the present

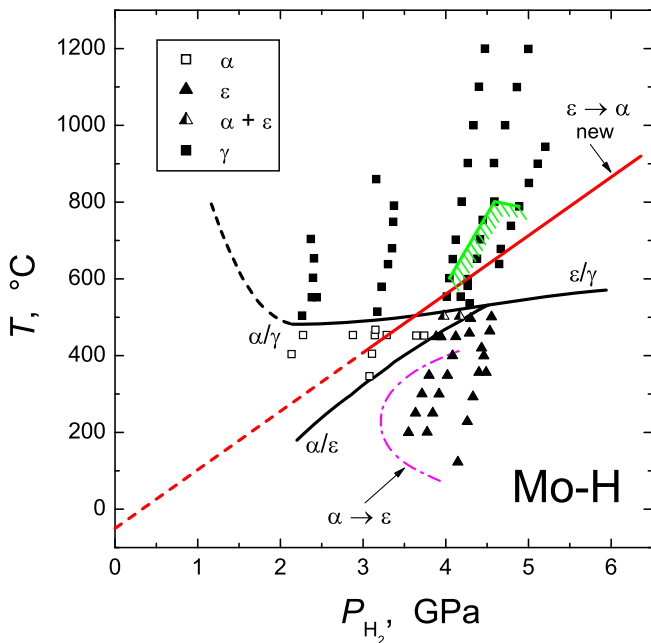


**Fig. 9.** The line of the  $\epsilon \rightarrow \alpha$  transition constructed in the present paper (straight line labeled “ $\epsilon \rightarrow \alpha$  new”) and the curve of the  $\alpha \rightarrow \epsilon$  transition from Ref. [13] (dash-dot line) superimposed onto the  $T$ - $P$  diagram of the Mo–H system proposed in Ref. [3] and formed by the  $\alpha/\gamma$ ,  $\alpha/\epsilon$  and  $\epsilon/\gamma$  boundaries. The boundaries are drawn on the basis of results of in situ X-ray diffraction measurements indicated by the symbols. The X-ray data was collected in a few series of heating runs at a constant ram load. The open squares and filled triangles stay for the single-phase samples of, respectively, dilute  $\alpha$  solutions and  $\epsilon$  hydrides. The filled squares indicate the presence of the  $\gamma$  phase. The hatched line represents the lower boundary of persistence of  $\epsilon$  hydride in the  $\gamma$  samples studied in Ref. [3] (see text).

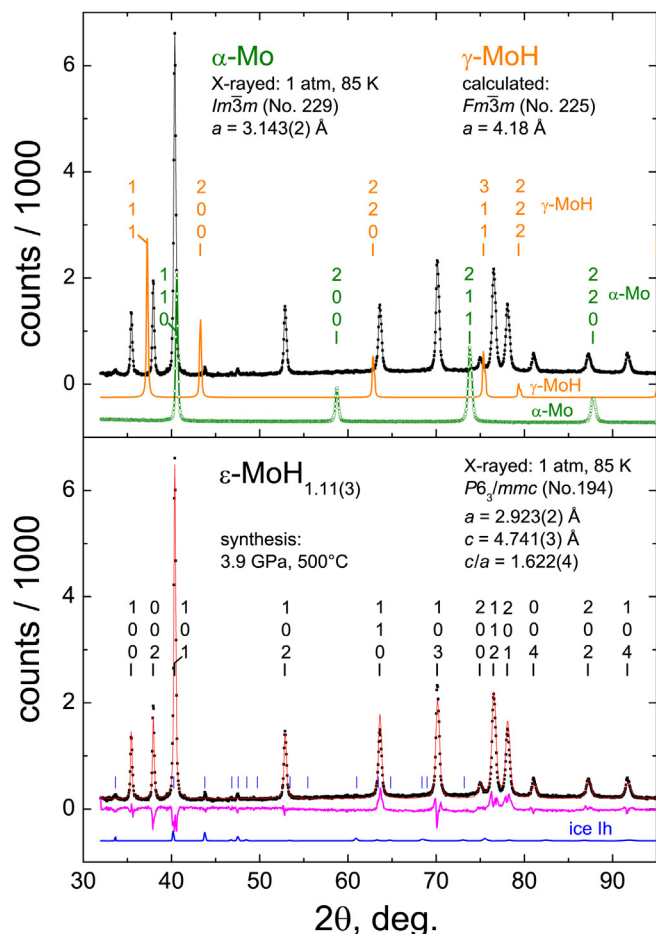


**Fig. 10.** Bottom panel: X-ray diffraction pattern of a  $\epsilon$ -MoH<sub>1.11</sub> sample quenched from 3.9 GPa to 500 °C (dots) and results of its profile analysis (downright: the fitting curve, the difference curve and the contribution from ice condensed on the sample during its loading into the X-ray cryostat). Upper panel: The experimental diffraction pattern of MoH<sub>1.11</sub> in comparison with the experimental pattern of the initial bcc ( $\alpha$ ) molybdenum and calculated pattern of the hypothetical fcc ( $\gamma$ ) MoH hydride with the lattice parameter  $a = 4.18$  Å estimated from the difference  $\Delta V_{\alpha \rightarrow \gamma} = 2.7$  Å<sup>3</sup>/atom Mo between the atomic volumes of  $\gamma$ -MoH and  $\alpha$ -Mo indicated in Ref. [3]. The  $\epsilon$ -MoH<sub>1.11</sub> sample was powdered in an agate mortar under liquid N<sub>2</sub>; the  $\alpha$ -Mo sample was produced by outgassing this powder in vacuum at 650 °C.

paper *i*) excluded formation of the fcc ( $\gamma$ ) MoH hydride at  $T > 480$ – $570$  °C and  $P > 2$  GPa reported in Ref. [3] and *ii*) revealed a significant overestimation of the  $\epsilon \rightarrow \alpha$  transition pressure in Ref. [13] at temperatures above 300 °C. Possible explanations of the

resulting discrepancies are suggested and discussed.

## Acknowledgments

This work was supported by grant No. 14-02-01200 from the Russian Foundation for Basic Research and by the Program “The Matter under High Pressures” of the Russian Academy of Sciences.

## References

- [1] Y. Fukai, *The Metal-hydrogen System*, Springer, Berlin, 2005.
- [2] Y. Fukai, M. Mizutani, Phase diagram and superabundant vacancy formation in Cr-H alloys, *Mater. Trans.* 43 (5) (2002) 1079–1084.
- [3] Y. Fukai, M. Mizutani, The phase diagram of Mo-H alloys under high hydrogen pressures, *Mater. Trans.* 44 (7) (2003) 1359–1362.
- [4] V.E. Antonov, I.A. Sholin, Proving the contact rules for phase regions: Implications to phase diagrams of metal-hydrogen systems, *J. Alloys Compd.* 645 (2015) S160–S165.
- [5] V.E. Antonov, A.I. Beskrovnyy, V.K. Fedotov, A.S. Ivanov, S.S. Khasanov, A.I. Kolesnikov, M.K. Sakharov, I.L. Sashin, M. Tkacz, Crystal structure and lattice dynamics of chromium hydrides, *J. Alloys Compd.* 430 (2007) 22–28.
- [6] I.T. Belash, V.E. Antonov, E.G. Ponyatovskii, Synthesis of molybdenum hydride at high hydrogen pressure, *Dokl. Akad. Nauk. SSSR* 235 (2) (1977) 379–380 (in Russian).
- [7] K. Wakamori, S.M. Filipek, A. Sawaoka, Convenient method for the synthesis of rare-earth hydrides by the use of a conventional very high pressure apparatus, *Rev. Sci. Instrum.* 54 (10) (1983) 1410–1411.
- [8] L.G. Khvostantsev, V.N. Slesarev, V.V. Brazhkin, Toroid type high-pressure device: history and prospects, *High. Press. Res.* 24 (2004) 371–383.
- [9] P.A. Storozhenko, R.A. Svitsyn, V.A. Ketsko, A.K. Buryak, A.V. Ul'yanov, Ammineborane: Synthesis and physicochemical characterization, *Zh. Neorgan. Khim.* 50 (7) (2005) 1066–1071 [Engl. Trans. *Russian J. Inorg. Chem.* 50 (7) (2005) 980–985].
- [10] V.E. Antonov, I.T. Belash, A method of calibration of quasihydrostatic high pressure chambers, in: *Fizika i Tekhnika Vysokikh Davlenii (High-pressure Physics and Technology)*, vol. 1, Naukova Dumka, Kiev, 1980, pp. 96–100 (in Russian).
- [11] M. Yamakata, T. Yagi, W. Utsumi, Y. Fukai, In situ X-ray observation of iron hydride under high pressure and high temperature, *Proc. Jpn. Acad.* 68B (1992) 172–176.
- [12] I.O. Bashkin, V.E. Antonov, A.V. Bazhenov, I.K. Bdkin, D.N. Borisenko, E.P. Krinichnaya, A.P. Moravsky, A.I. Harkunov, YuM. Shul'ga, YuA. Ossipyan, E.G. Ponyatovskiy, Thermally stable hydrogen compounds obtained under high pressure on the basis of carbon nanotubes and nanofibers, *Zh. Eksp. Teor. Fiz. Pisma* 79 (5) (2004) 280–285 [Engl. Trans. *JETP Lett.* 79 (5) (2004) 226–230].
- [13] V.E. Antonov, I.T. Belash, E.G. Ponyatovskii, T-P phase diagram of the Mo-H system at temperatures to 500 °C and pressures to 50 kbar, *Dokl. Akad. Nauk. SSSR* 248 (3) (1979) 635–637 (in Russian).
- [14] V.E. Antonov, A.I. Latynin, M. Tkacz, T-P phase diagrams and isotope effects in the Mo-H/D systems, *J. Phys. Condens. Matter* 16 (46) (2004) 8387–8398.
- [15] M. Tkacz, A. Litwiniuk, Useful equations of state of hydrogen and deuterium, *J. Alloys Compd.* 330–332 (2002) 89–92.
- [16] A.V. Irodova, V.P. Glazkov, V.A. Somenkov, S.Sh. Shil'shtein, V.E. Antonov, E.G. Ponyatovskii, Neutron-diffraction investigation of structures of the hydrides of molybdenum, rhodium, and nickel, *Kristallografiya* 33 (3) (1988) 769–771 [Engl. Trans. *Sov. Phys. Crystallography* 33 (3) (1988) 453–455].
- [17] V.E. Antonov, I.T. Belash, E.G. Ponyatovskii, A method to produce high hydrogen pressure, in: *Fizika i Tekhnika Vysokikh Davlenii (High-pressure Physics and Technology)*, 9, Naukova Dumka, Kiev, 1982, pp. 65–72 (in Russian).